Critical Role of c-Jun N-Terminal Protein Kinase Activation in Troglitazone-Induced Apoptosis of Human HepG2 Hepatoma Cells

MYUNG-AE BAE and BYOUNG J. SONG

Laboratory of Membrane Biochemistry and Biophysics, National Institute on Alcohol Abuse and Alcoholism, National Institutes of Health, Rockville, Maryland

ABSTRACT

The peroxisome proliferator-activated receptor agonist troglitazone (TRO) was used for treatment of non–insulin-dependent diabetes until its removal from the market because of its severe hepatotoxicity. However, the mechanism for its hepatotoxicity is still poorly understood. In this study, we investigated whether TRO caused cell death by altering signaling pathways associated with cell damage and survival in human hepatoma cells. Our data reveal that TRO caused time- and concentration-dependent apoptosis of HepG2 and Chang liver human hepatoma cells, as evidenced by DNA fragmentation and staining with Hoechst 33342. In contrast, 50 or 100 μM rosiglitazone, a structural analog of TRO, did not cause apoptosis in these hepatoma cells. TRO activated both c-Jun N-terminal protein kinase (JNK) and p38 kinase about 5-fold between 0.5 and 8 h before they returned to control levels at 16 h in HepG2 cells. In contrast, TRO failed to activate the extracellular signal-regulated kinase. Furthermore, TRO increased the levels of proapoptotic proteins, Bad, Bax, release of cytochrome c, and cleavage of Bid in a time-dependent manner. The antiapoptotic Bcl-2 protein level decreased in hepatoma cells treated with TRO. Pretreatment of hepatoma cells with a selective JNK inhibitor, anthra[1,9-cd]pyrazol-6(2H)-one (SP600125), significantly reduced the rate of TRO-induced cell death, whereas 4-(4-fluorophenyl)-2-(4-methylsulfinylphenyl)-5-(4-pyridyl)-1H-imidazole (SB203580), an inhibitor of p38 kinase, had little effect on apoptosis. Pretreatment with SP600125 also prevented JNK activation and c-Jun phosphorylation. In addition, rosiglitazone, which is not as toxic to hepatoma cells as TRO, did not stimulate JNK activity. Transfection of cDNA for the dominant-negative mutant JNK-KR (Lys→Arg) or SEK1-KR (Lys→Arg), an immediate upstream kinase of JNK, significantly reduced TRO-induced JNK activation and cell death rate. Furthermore, SP600125 pretreatment effectively prevented the TRO-mediated changes in Bad, Bax, Bid cleavage, and cytochrome c release. These data strongly suggest that hepatotoxic TRO causes apoptosis by activating the JNK-dependent cell death pathway accompanied by increased Bid cleavage and elevation of proapoptotic proteins.

Troglitazone (TRO; Rezulin), a thiazolidinedione compound, is a novel antidiabetic agent that was originally approved to treat patients with adult-onset non–insulin-dependent diabetes. TRO is an agonist of the peroxisome proliferator-activated receptor γ (PPARγ) (Lehmann et al., 1995; Mahler and Adler, 1999) that sensitizes target cells to insulin, thereby improving the metabolic conditions associated with adult-onset diabetes. Although the precise mechanism of action of TRO is still not fully understood, the insulin-sensitizing effects of TRO are believed to be mediated through the activation of PPARγ. This notion is supported by the fact that the binding affinity of TRO analogs to PPARγ corresponds to the potency of their anti-diabetic action (Wil-

son et al., 1996; Beales et al., 1998; Day, 1999; Lebovitz et al., 2002).

Despite the many benefits of TRO, it is known to also induce apoptosis in experimental animal models (Ohtani et al., 1998; Keelan et al., 1999). In addition, during preclinical trials and clinical use, approximately 1.9% of patients developed severe hepatic problems with elevated serum transaminase activities (Watkins and Whitcomb, 1998). In some severe cases, TRO caused fulminant hepatic failures, leading to multiple human deaths. Because of severe side effects of TRO and the availability of its structural derivatives such as rosiglitazone (RSG) and pioglitazone (Day, 1999), TRO was removed from the market in 2000. However, the mechanism by

---

ABBREVIATIONS: TRO, troglitazone; PPAR, peroxisome proliferator-activated receptor; RSG, rosiglitazone; ERK, extracellular signal-regulated kinase; JNK, c-Jun N-terminal protein kinase; p38 kinase, p38 mitogen activated protein kinase; MAP, mitogen-activated protein; DMSO, dimethyl sulfoxide; MTT, 3-[4,5-dimethylthiazol-2-yl]-2,5-diphenyl tetrazolium bromide; ATF, activator transcription factor; wt, wild type; SEK, stress activated protein kinase kinase; JNK-KR, c-Jun N-terminal protein kinase Lys→Arg mutant; SEK1-KR, stress activated protein kinase kinase 1 Lys→Arg mutant; SP600125, anthra[1,9-cd]pyrazol-6(2H)-one; SB203580, 4-(4-fluorophenyl)-2-(4-methylsulfinylphenyl)-5-(4-pyridyl)-1H-imidazole.

which TRO induces liver damage or hepatotoxicity is poorly understood. TRO-induced apoptosis does not seem to be mediated through PPARγ activation, because other structural analogs of TRO, such as RSG and pioglitazone, both of which stimulate the PPARγ, do not seem to cause increased cell death (Day, 1999; Lebovitz et al., 2002).

Extracellular signal-regulated kinase (ERK) plays an important role in cell proliferation, differentiation, and survival promoted by many endogenous and exogenous growth stimuli (Karin, 1995). On the other hand, various pro-inflammatory cytokines, removal of growth factors, chemotherapeutic agents and many toxic compounds usually stimulate the activities of c-Jun N-terminal protein kinase (JNK) or stress-activated protein kinase and p38 mitogen-activated protein kinase (p38 kinase), leading to cell death. It is also known that these mitogen-activated protein (MAP) kinases are often regulated in an opposing manner upon exposure to exogenous factors or toxicants (Xia et al., 1995). To our knowledge, the effects of TRO on these MAP kinases and their roles in TRO-induced apoptosis have not been studied systematically. Therefore, in this study, we investigated the effects of TRO on various proteins involved in the early signaling pathway and apoptosis-related proteins in human hepatoma cells.

Materials and Methods

Materials. Dimethyl sulfoxide (DMSO; tissue culture grade), trypan blue, bromphenol blue, and ethidium bromide were purchased from Sigma Chemicals (St. Louis, MO). TRO was kindly provided by Parke-Davis Company (Ann Arbor, MI) and Dr. Herman Rhee (US Food and Drug Administration, Rockville, MD). RSG was kindly provided from Dr. Joong-Kwon Choi (Korea Research Institute of Chemical Technologies, Daejon, Korea). All tissue culture media, including fetal bovine serum, antibiotics, and trypsin were purchased from Invitrogen (Carlsbad, CA). SP600125, SB203580, and Hoechst 33342 were from Calbiochem (San Diego, CA). Specific antibodies to the proteins analyzed were purchased from Santa Cruz Biotechnologies (Santa Cruz, CA).

Hepatoma Cell Culture and Determination of Cell Viability. HepG2 and Chang liver human hepatoma cells, and McA-RH7777 rat hepatoma cells were purchased from American Type Culture Collection (Manassas, VA) and maintained in minimal essential medium with Earl's salts, 10% (v/v) fetal bovine serum, 100 IU/ml penicillin, and 100 μg/ml streptomycin in a humidified incubator under 5% CO_2/95% air at 37°C. HepG2 and Chang liver cells, grown in 96-well microtiter plates (1×10^4 cells/well) for 2 days, were incubated with varying concentrations of TRO or RSG (diluted in DMSO at 0.05% final concentration) for different times. Cell viability was measured by using MTT (3-[4,5-dimethylthiazol-2-yl]-2,5-diphenyl tetrazolium bromide) as a substrate. Trypan blue dye exclusion assay was performed to confirm and verify cell viability.

Detection of DNA Fragmentation by Agarose Gel Electrophoresis. High-molecular-weight DNA was isolated from TRO-treated HepG2 cells (5×10^6 cells/culture flask) and analyzed by agarose gel electrophoresis as described recently (Bae et al., 2001).

Immunoblot Analyses. HepG2 cells, grown in a culture flask (150-mm diameter), were treated with TRO for different times and harvested by centrifugation at 3000g for 5 min at 4°C. The levels of JNK, p38 kinase, ERK, Bax, Bad, cytochrome c release, Bcl-2, phospho-JNK, phospho–c-Jun, and phospho-stress activated protein kinase kinase (SEK) were determined by immunoblot analysis as described previously (Bae et al., 2001). Briefly, whole cell lysates were separated on SDS-polyacrylamide gels, electrically transferred onto nitrocellulose membranes, and then incubated with polyclonal antibodies against the target proteins followed by incubation with a secondary antibody. The bound antigen-antibody complexes were finally recognized by enhanced chemiluminescence detection with a SuperSignal West Pico ECL detection kit (Pierce Chemicals, Rockford, IL).

Measurement of JNK, p38 Kinase, and ERK Activities. HepG2 cells, grown in culture flasks (150-mm diameter) and treated with TRO for indicated times, were harvested and homogenized in ice-cold lysis buffer, as described previously (Soh et al., 2000). The activity of specific MAP kinases in the soluble extracts was determined by using activator transcription factor-2 (ATF-2) or myelin basic protein as a substrate (Soh et al., 2000). The whole-cell extracts (300 μg of protein/reaction) were incubated with polyclonal antibodies to JNK, p38 kinase, and ERK, respectively, for 2 h followed by incubation with protein A-agarose beads for an additional 2 h at 4°C. The immunoprecipitated protein was washed with the lysis buffer three times before washing with the kinase buffer twice. The protein kinase reaction buffer contained: 20 mM Tris-HCl, pH 7.5, 20 mM $MgCl_2$, 5 mM EGTA, 0.5 mM dithiothreitol, 0.1 μg myelin basic protein or ATF-2, 30 μM ATP, and 10 μCi of [^{32}P]ATP. After incubation for 15 min at 37°C, the enzyme reaction was terminated by adding 2× SDS sample buffer. The samples were separated on a 10% SDS-polyacrylamide gel, visualized by staining, and processed for autoradiography. Alternatively, activation of each MAP kinase was also determined by immunoblot analysis using the antibody that specifically recognizes the phosphorylated form of each MAP kinase.

Transient Expression of Various cDNAs. The respective cDNA construct (8 μg each) for JNK wild type (wt), SEK1 wt, JNK-KR (Lys→Arg), or SEK1-KR (Lys→Arg) dominant-negative mutant was transfected into HepG2 cells (60–70% confluence; grown on 6-cm culture dishes), using LipofectAMINE 2000 reagent according to the manufacturer's instruction, as described previously (Soh et al., 2000; Bae et al., 2001). The level of protein expressed after transfection of the respective cDNA was also determined by immunoblot analysis using the specific antibody toward each target protein.

Statistical Analysis. Experimental results shown were repeated two or three times, unless otherwise indicated. Results are expressed as means ± S.E.M. The mean values were compared using Student's t test. $P < 0.05$ value is considered statistically significant. Other methods not described in this report were as same as described previously (Soh et al., 2000; Bae et al., 2001)

Results

Time- and TRO Concentration-Dependent Apoptosis of Human Hepatoma Cells. To evaluate the cytotoxic effects of TRO on cultured hepatoma cells, we treated HepG2 and Chang liver cells with varying concentrations of TRO for different times and measured the cell viability by trypan blue exclusion or the reduction of MTT. TRO caused cell death of HepG2 and Chang liver cells in a time- and concentration-dependent manner (Fig. 1). At 5 and 25 μM TRO, about 10 to 20% of HepG2 and Chang liver cells died after 24 h of treatment, whereas very few cells died (<1%) in the DMSO-treated control. Between 20 and 40% of cells died after exposure to 50 and 100 μM TRO, respectively, at 24 h; more cells (41–87%) died at 48 h. The morphology of TRO-treated hepatoma cells changed considerably, whereas the DMSO-treated control remained the same (data not shown). Cells treated with 50 μM TRO for 36 h showed cell shrinkage, rounding, and partial detachment along with the lobulated appearance of apoptotic cells (data not shown) and by staining with Hoechst 33342 (data not shown). Fluorescence-activated cell sorting analysis revealed that TRO increased the population of cells under sub-G_1 stage (20.9% at 24 h and 40.1% at 48 h) compared with DMSO-treated control (1.2%).
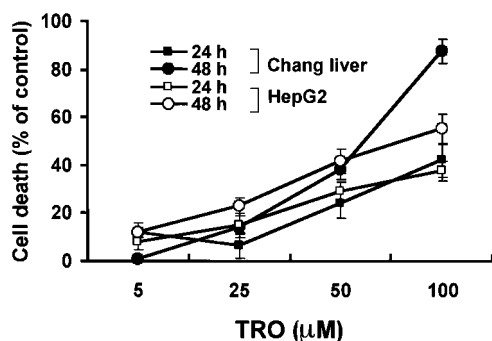
Fig. 1. Time- and TRO concentration-dependent cell death. HepG2 and Chang liver hepatoma cells, grown in 96-well microplates, were exposed to different concentrations of TRO as indicated. Cell viability was determined 24 and 48 h after TRO exposure by the reduction of MTT. Results represent the average ± S.E.M. from three to five different experiments.

In contrast, RSG did not change the population of the sub-G_1 stage (1.9% at 48 h).

Very little DNA fragmentation, a hallmark of apoptosis, was observed when HepG2 cells were treated with 1 or 25 μM TRO for 36 h but was clearly visible after treatment with 50 or 100 μM TRO (Fig. 2A). In addition, DNA fragmentation was time-dependent. Apoptosis was not evident at 12 h but was clearly visible at 24, 36, and 48 h after hepatoma cells were exposed to 50 μM TRO (Fig. 2B), further supporting TRO-induced apoptosis of HepG2 cells.

TRO-Induced Activation of JNK and p38 Kinase in HepG2 Cells. To study the early signaling mechanism during TRO-induced apoptosis of hepatoma cells, we investigated changes in the activity of the three MAP kinases: JNK, p38 kinase, and ERK1 in HepG2 cells by immuno-complex
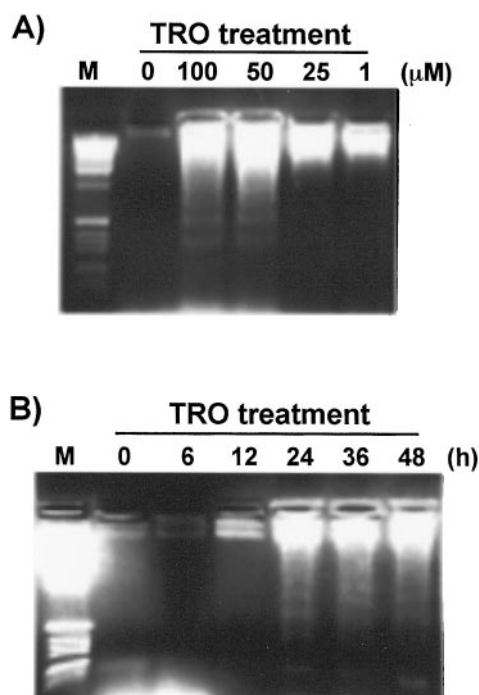

Fig. 2. Effects of TRO on DNA fragmentation in HepG2 cells. Exponentially growing HepG2 cells were collected to assess DNA fragmentation after exposure to different concentrations of TRO for 24 h (A) or for different times after exposure to 50 μM TRO (B). DNA prepared from each group was subjected to electrophoresis on 1.8% agarose gel and visualized with ethidium bromide.

kinase assay. As shown in Fig. 3A, TRO treatment resulted in a time-dependent activation of JNK1 and p38 kinase in HepG2 cells, as indicated by the increased phosphorylation of ATF-2 protein. JNK1 and p38 kinase activation reached a maximal level (5-fold) after 4 h of TRO exposure in HepG2 cells. In contrast, TRO did not change the ERK1 activity in HepG2 cells (data not shown). Immunoblot analyses verified that the levels of JNK, p38 kinase, and ERK protein did not change during TRO treatment (data not shown). These results suggest that the elevation of JNK and p38 kinase activities stem not from the increased expression of JNK and p38 kinase proteins but from phosphorylation. Consistent with the JNK activation, TRO also activated (phosphorylated) SEK1, the immediate upstream kinase of JNK, in a time-dependent manner in HepG2 cells (Fig. 3B) and McA-RH7777 cells (data not shown). Given the lack of change in the ERK1 activity, the elevation of both JNK1 and p38 kinase activity seems to be important in TRO-mediated apoptosis of HepG2 cells. TRO-induced JNK activation (phosphorylation) was also observed in two other hepatoma cell lines (Fig. 3C), similar to that observed in HepG2 cells.

TRO-Induced Changes in the Levels of Apoptosis-Related Proteins. Levels of proapoptotic Bax and antiapoptotic Bcl-2 proteins and their ratios are considered critical factors in initiation of apoptosis (Chao and Korsmeyer, 1998). Therefore, we determined the levels of proapoptotic Bax and its antiapoptotic counterpart, Bcl-2, by immunoblot analysis (Fig. 4A). TRO significantly increased the level of Bax and strikingly reduced the level of Bcl-2 at 24 h (Fig. 4A). In fact,
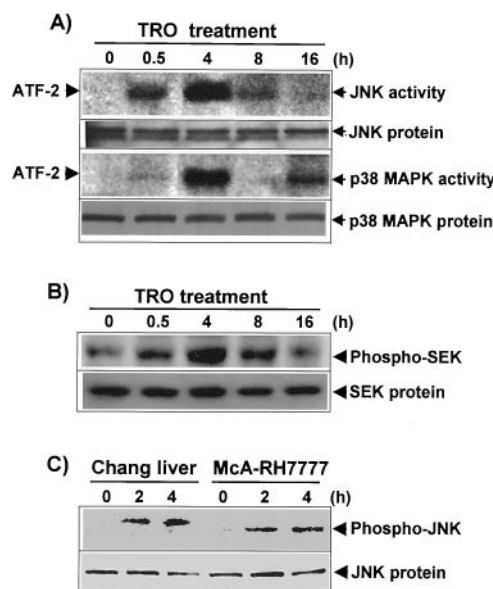

Fig. 3. Time-dependent activation of JNK and p38 kinase by TRO in hepatoma cells. A, HepG2 cells were treated with 50 μM TRO for 0, 0.5, 4, 8, and 16 h. Whole-cell extracts (300 μg of protein/measurement) prepared at different time points were subjected to measurement of JNK or p38 kinase activity. Catalytic activity and its protein level of each kinase were determined by immunocomplex assay and immunoblot analyses, respectively, as described under *Materials and Methods*. B, whole cell extracts (300 μg of protein/lane) of HepG2 cells treated with TRO for different time points were subjected to 10% SDS-PAGE followed by immunoblot analyses using the specific antibody against phospho-SEK or SEK protein. C, Chang liver or McA-RH7777 hepatoma cells were treated with 50 μM TRO for 0, 2, and 4 h. The whole-cell extracts (300 μg of protein/lane) were then subjected to 10% SDS-PAGE followed by immunoblot analyses using the specific antibody against phospho-JNK or JNK protein.
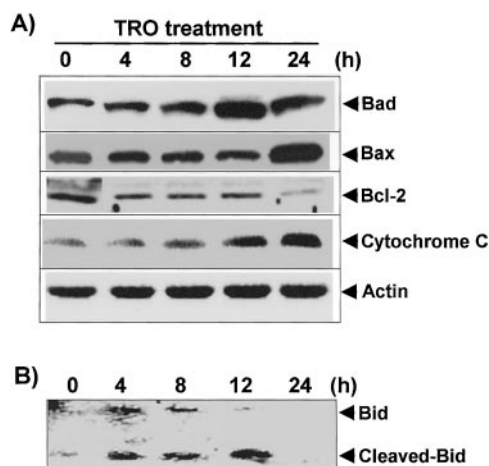
A)

B)

Fig. 4. Immunoblot analysis for expression of apoptosis-related proteins. Exponentially growing HepG2 cells were exposed to 50 μM TRO for the indicated times and cells were then harvested. A, whole cell extracts (100 μg protein/lane) were separated on 14% SDS-polyacrylamide gels followed by immunoblot analyses. Each target protein band was detected with the respective antibody against Bad, Bax, Bcl-2, cytochrome *c*, or actin protein. B, levels of Bid and cleaved Bid protein were also determined by immunoblot analysis.
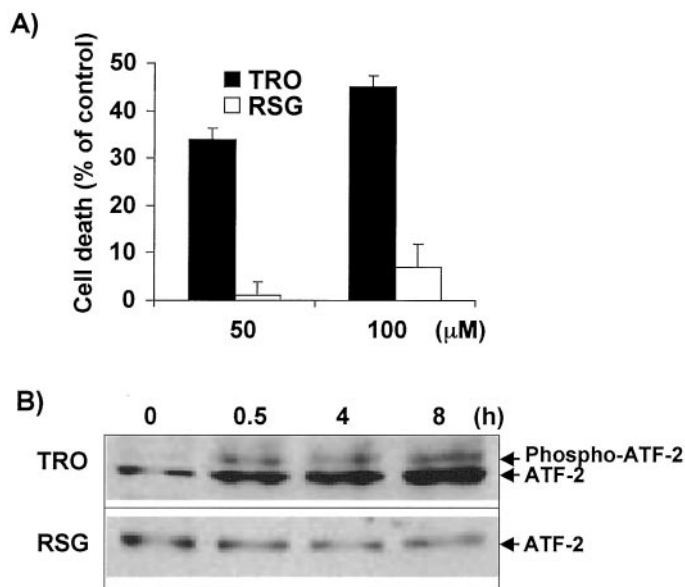
A)

B)

Fig. 5. Differential effects of TRO and RSG on cell death rate and JNK activation. A, HepG2 cells, grown in microtiter plates, were exposed to 50 μM TRO or RSG for 24 h. The rate of cell death was determined by the method described in Fig. 1 legend. B, exponentially growing HepG2 cells were exposed to 50 μM TRO or RSG for 0, 0.5, 4, and 8 h before they were harvested by centrifugation. Whole-cell extracts (300 μg of protein/lane) were separated on 10% SDS-polyacrylamide gels. JNK activation was determined by immunoblot analysis using the antibody against phospho-ATF-2 protein, which also recognizes the unphosphorylated ATF-2 protein.

the densitometric ratio of Bax/Bcl-2 increased more than 10-fold at 24 h after TRO treatment compared with the untreated control cells. Consistent with these changes, the levels of other apoptosis-related proteins such as Bad and cytochrome *c* were also increased in a time-dependent manner after TRO exposure of HepG2 cells (Fig. 4A).

TRO-Induced Cleavage and Translocation of Bid Protein. It is well established that JNK activation may be

involved in Bid cleavage, and its translocation into mitochondria (Tournier et al., 2000), before initiation of apoptosis (Slee et al., 2000). Therefore, we determined whether TRO caused Bid cleavage and mitochondrial translocation. Our results show a time-dependent cleavage of the mitochondrial Bid protein. Increased cleavage of Bid protein was observed at 4, 8, and 12 h and was no longer detected 24 h after TRO treatment of HepG2 cells (Fig. 4B).

Critical Role of JNK Activation in TRO-Mediated Apoptosis. Our results suggest that TRO causes apoptosis of HepG2 cells via JNK activation and Bid cleavage. To determine whether a correlation between cell death and JNK activation exists, we studied the effect of RSG, a structural analog of TRO, on JNK activation and cell death in hepatoma cells. As shown in Fig. 5A, TRO caused apoptotic cell death of HepG2 cells in a concentration-dependent manner. However, 50 or 100 μM RSG did not cause significant damage to HepG2 cells after 24 h of exposure. In addition, 100 μM RSG did not cause damage to McA-RH7777 rat hepatoma cells (data not shown), suggesting that RSG is not as toxic to hepatoma cells as TRO. Furthermore, TRO increased the JNK activity as measured by phosphorylation of ATF-2 at 0.5, 4, and 8 h. In contrast, RSG did not activate JNK activity at any time in HepG2 cells (Fig. 5B).

To further demonstrate the role of JNK activation in TRO-mediated apoptosis, we also studied the effects of the respective inhibitor of JNK (SP600125; Bennett et al., 2001) or p38 kinase (SB203580; Lee et al., 1994) on cell death and JNK activation. We first confirmed that SP600125 pretreatment markedly blocked JNK activation and the phosphorylation of c-Jun (Fig. 6B). We then tested the effect SP600125 on TRO mediated cell death. Less than 10% of cells died after exposure to either SP600125 or SB203580 alone, whereas about 36% cells died after treatment with 50 μM TRO for 24 h (Fig. 6A). SP600125 pretreatment significantly reduced the rate of TRO-mediated cell death, whereas SB203580 did not prevent TRO-mediated cell death. These results indicate an important role of JNK activation and c-Jun phosphorylation in TRO-mediated cell death.

To further investigate the critical role of the JNK activation in TRO-induced cell damage, HepG2 cells were transiently transfected with the cDNA for JNK wt, SEK1 wt, JNK-KR, or SEK1-KR dominant-negative mutant, followed by measurements of JNK or SEK activity and relative cell death rates upon TRO exposure. The transfection efficiency of each cDNA, determined by the method (Bae et al., 2001), ranged from 8 to 12% of total HepG2 cells. JNK was activated (phosphorylated) minimally without TRO treatment (Fig. 7A, top, lane 1). Consistent with the data in Figs. 3, 5, and 6, TRO treatment significantly increased JNK activity in HepG2 cells transfected with the pcDNA vector alone (lane 2). In this system, transfection of the wild-type JNK (lane 4) or SEK1 cDNA (lane 6) further increased JNK activity over the TRO-induced JNK activation (top, lane 2). However, transfection of the cDNA for JNK-KR or SEK1-KR dominant-negative mutant markedly decreased the JNK or SEK1 activity after exposure to TRO (Fig. 7A, top and second blots, lanes 3 and 5), compared with their respective counterpart. The expression of transduced JNK or SEK1 protein was verified by immunoblot analysis (Fig. 7A, third and fourth blots). These results indicate that TRO increased JNK activity through the

SEK1-JNK pathway, consistent with the data shown in Fig. 3.

The functional role of JNK activation was also investigated by measuring the rate of cell death, after transient transfection of the same set of cDNAs and then exposure to 50 μM TRO for additional 24 h, before cell viability assay. Less than 3% of HepG2 cells died in DMSO vehicle control when cells were transfected with the pcDNA vector alone (data not shown). Approximately 40% of HepG2 cells died after TRO exposure (Fig. 7B, lane 1). In contrast, 57 or 48% of cells died when cDNA for JNK wt or SEK1 wt was transfected and then exposed to TRO (lanes 2 and 4). However, the rate of cell death was significantly reduced by transfecting cDNA for the dominant-negative mutant, JNK-KR (28%, lane 3) or SEK1-KR (27%, lane 5), compared with its wild-type counterpart. These data clearly establish a critical role of JNK and SEK1 activation in TRO-induced cell death.

Effect of SP600125 on TRO-Induced Changes in the Levels of Apoptosis-Related Proteins. To further demonstrate the role of JNK activation in TRO-induced cell death, we evaluated the effect of JNK inhibition by SP600125 on TRO-induced changes in the levels of apoptosis-related proteins. As shown in Fig. 8, pretreatment of HepG2 cells with SP600125 effectively prevented the TRO-induced changes in the levels of Bax, Bad, Bcl-2, and cytochrome c release in a time-dependent manner. In addition, TRO-induced Bid

cleavage was also blocked by the JNK inhibition with SP600125. These data also support the idea that JNK activation plays an important role in TRO-induced apoptosis of hepatoma cells.

Effect of Cycloheximide on TRO-Induced Cell Death Rate. To study whether TRO-induced cell death is mediated
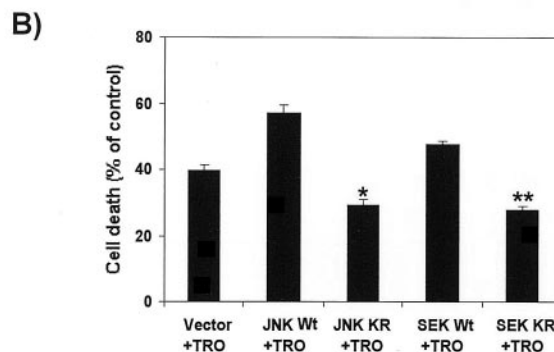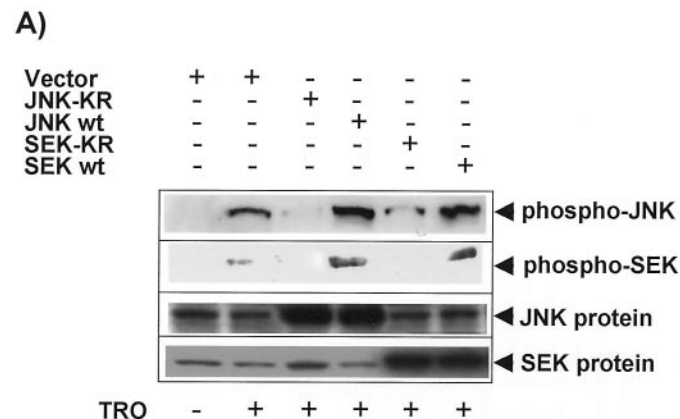
Fig. 7. Critical role of the JNK activation in TRO-induced cell death. A, the expression vector containing the cDNA for SEK1 wt, JNK wt, SEK1-KR, or JNK-KR dominant-negative mutant as indicated was transiently transfected into HepG2 cells for 48 h. Cells were then treated with 50 μM TRO for 4 h, harvested, homogenized, and subjected to measurement of JNK or SEK1 activation using the antibody against their respective phospho-JNK (top) or phospho-SEK1 protein (second blot). Immunoblot results also represent the relative level of transduced JNK or SEK1 protein (third and fourth blots). B, HepG2 cells (2×10^4 cells/well), grown in 96-well microtiter plates, were transiently transfected with 0.2 μg of each construct as indicated and treated with 50 μM TRO for additional 24 h. Cell viability was then measured by the MTT reduction method. Asterisks indicate significant difference ($p < 0.05$) from the corresponding JNK wt (⋆) and SEK1 wt (⋆⋆).
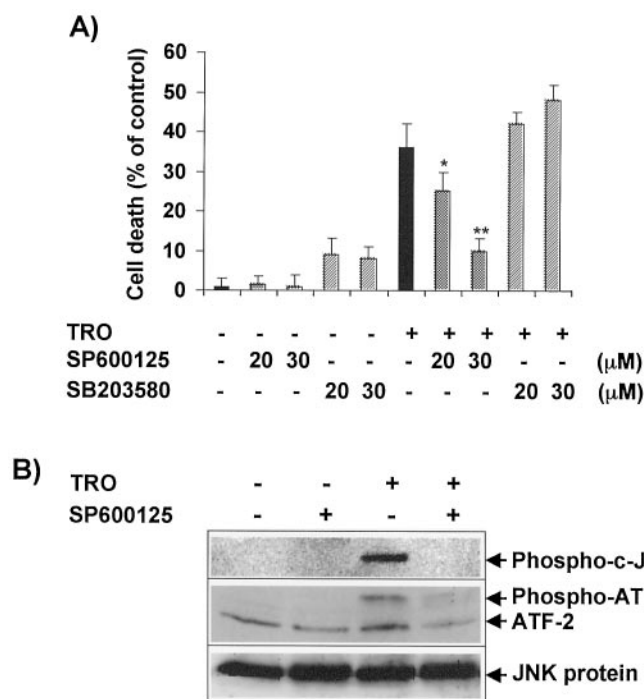
Fig. 6. Differential effects of SP600125 and SB203580 on the rate of cell death, c-Jun phosphorylation and JNK activity. A, HepG2 cells, grown in microtiter plates, were pretreated with DMSO (control) and 20 or 30 μM SB203580 or SP600125 for 3 h, as indicated, before exposure to 50 μM TRO for additional 24 h. Cell viability was then determined by the MTT viability assay. Results represent the average ± S.E.M. from five different experiments. Significantly different (*, $p < 0.05$; **, $p < 0.01$) from the TRO-treated samples. B, exponentially growing HepG2 cells were pretreated with 30 μM SP600125 for 3 h and then treated with 50 μM TRO for additional 4 h before cells were collected by centrifugation. Immunoblot analyses were performed by using the specific antibody against phosphorylated c-Jun, phospho-ATF-2 (JNK activation), or JNK protein, as described in Fig. 5 legend.
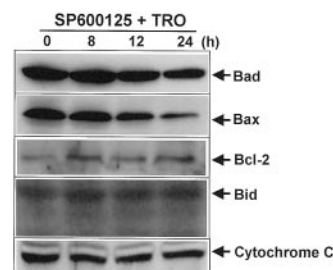
Fig. 8. Effects of SP600125 on TRO-induced changes in the levels of apoptosis-related proteins. HepG2 cells were pretreated with 30 μM SP600125 for 3 h and then treated with 50 μM TRO for additional times as indicated before cells were collected by centrifugation. Immunoblot analyses were performed by using the specific antibody against Bad, Bax, Bcl-2, Bid, and cytochrome c, as described in Fig. 4 legend.

through de novo protein synthesis after JNK activation, HepG2 cells were pretreated with an inhibitor of protein synthesis, cycloheximide, for 6 h, before treatment with TRO for additional 24 h before assaying for cell death. As shown in Fig. 9, approximately 40% of HepG2 cells died upon exposure to TRO alone, whereas about 5 and 17% cells died after treatment with 10 and 50 μM cycloheximide alone. However, cycloheximide pretreatment did not significantly alter the rate of cell death caused by TRO in the presence of cycloheximide. These results indicate that new protein synthesis does not seem to play a major role in TRO-induced cell damage.

Discussion

Troglitazone, a previously popular drug for treating patients with adult-onset diabetes, was removed from the market because of severe hepatotoxicity and the concurrent availability of structural analogs (RSG and pioglitazone) with reduced toxicities (Watkins and Whitcomb, 1998; Day, 1999; Lebovitz et al., 2002). TRO was shown to causes apoptosis of many different cell lines including: endothelial cells, monocyte-derived macrophages (Chinetti et al., 1998), six colon cell lines (Kitamura et al., 1999), HL60 promyelocytic leukemia cells (Hirase et al., 1999), and vascular smooth muscle cells (Okura et al., 2000). TRO was recently shown to induce apoptosis in human liver cancer cells (Toyoda et al., 2001, 2002). However, the mechanism by which TRO induces apoptosis is not well established. In particular, the role of the MAP kinases in TRO-induced apoptosis has not been studied systematically in these studies. Therefore, we investigated the signaling mechanism and its role during TRO-induced apoptosis in cultured hepatoma cells. We used HepG2, Chang liver, or McA-RH7777 hepatoma cells as our model systems, because these cells undergo apoptosis upon exposure to TRO, similar to the human and porcine primary hepatocyte systems, as recently reported (Ramachandran et al., 1999; Kostrubsky et al., 2000). Our results reveal that TRO treatment activates JNK and p38 kinase long before the initiation of apoptosis and thus provides a strong link between the JNK/ stress-activated kinase pathway and hepatic cell death induced by TRO.

Gouni-Berthold et al. (2001) recently reported that both TRO and RSG cause apoptosis of vascular smooth muscle cells. In that study, RSG was about 10-fold more effective in causing apoptosis than TRO. However, our current data indicates that TRO was much more toxic than RSG, because 100 μM RSG did not cause significant damage to HepG2 or McA-RH7777 hepatoma cells. We do not know the reason for the apparent differences in cell responses after treatment with RSG or TRO, but our results are similar to the pattern of differential apoptosis in rat hepatocytes caused by TRO and RSG (Toyoda et al., 2001 and 2002) as well as the clinical results of human liver toxicity between TRO and RSG (Mahler and Adler, 1999; Lebovitz et al., 2002).

Our data demonstrated that hepatoma cells died mainly by apoptosis after exposure to 25 or 50 μM TRO, a dose similar to that used in other studies (Kitamura et al., 1999). TRO increased the activities of JNK and p38 kinase followed by elevated levels of proapoptotic proteins: Bad, Bax, and cytochrome *c* with an opposing reduction in the level of antiapoptotic Bcl-2 protein. These data suggest that sustained activation of JNK and p38 kinase up to 8 h may play a key role in the TRO-induced apoptosis of HepG2 hepatoma cells. Our data also suggest that activation of p38 kinase may not be as important as JNK activation because the inhibitor of p38 kinase, SB203580 at 20 or 30 μM, did not change the rate of TRO-induced cell death. In contrast, pretreatment with the inhibitor of JNK (SP600125 at 20 or 30 μM) significantly reduced the cell death rate, JNK activation, and c-Jun phosphorylation. Furthermore, SP600125 pretreatment effectively prevented the TRO-induced changes in the levels of various apoptosis-related proteins such as Bax, Bad, Bid cleavage, and cytochrome *c* release. In contrast, 100 μM RSG, which did not cause damage to HepG2 or MCR7777 hepatoma cells under our experimental conditions, did not activate the JNK. Transfection of dominant-negative JNK-KR or SEK1-KR mutant not only blocked JNK activation but also significantly changed the rate of TRO-mediated cell death. All these results strongly indicate the important role of the JNK-related pathway in TRO-mediated cell death.

The critical role of JNK-mediated signaling pathway in cell death is actively being studied in many model systems. Many toxic compounds, serum removal, γ-ray irradiation, UV exposure, and proinflammatory cytokines cause cell damage by activating the JNK-mediated cell death pathway (Karin, 1995; Xia et al., 1995; Chen et al., 1996). Many investigators have demonstrated this concept in various experimental model systems using different experimental tools: antisense oligonucleotides to JNK (Daily et al., 2001), transfection of dominant-negative cDNA for JNK and SEK1, immediate upstream protein kinase of JNK (Soh et al., 2000), chemical inhibitors of JNK (Maroney et al., 1999), JNK knock-out mice or cells (Tournier et al., 2000), as well as others. However, how JNK activation actually leads to cell death remains unknown, although several mechanisms are being proposed. For instance, JNK activation may lead to up-regulation of c-Jun and Fas ligand (Le-Niculescu et al., 1999), ceramide production (Engedal and Saatcioglu, 2001), Bid cleavage and translocation before cytochrome *c* release (Tafani et al., 2002), and alteration of Ca^{2+} homeostasis (Inanami et al., 1999) before activation of caspases and actual cell damage.
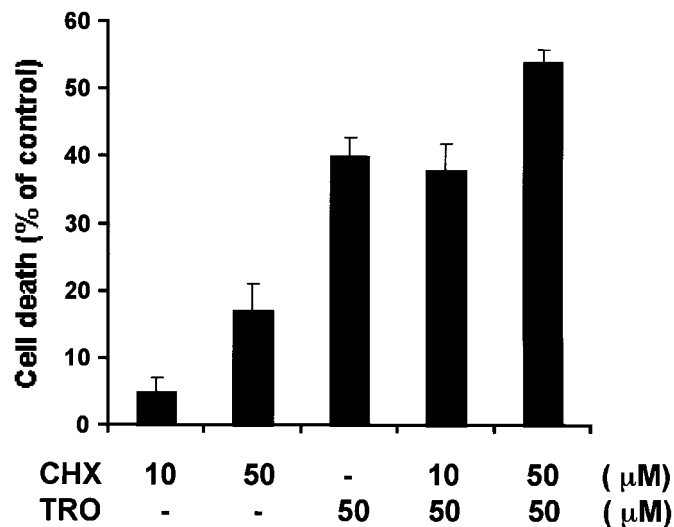

Fig. 9. Effects of cycloheximide on TRO-induced cell death rate. HepG2 cells were pretreated with 10 or 50 μM cycloheximide (CHX) for 6 h and then treated with 50 μM TRO for additional 24 h before cell death rate was determined by the MTT reduction assay.

Our data showed that JNK activation took place simultaneously or before the up-regulation of proapoptotic proteins Bax, Bad, Bid cleavage, and cytochrome *c* release. These results are consistent with the recent report indicating a key role of Bid cleavage and cytochrome *c* release before apoptosis (Tafani et al., 2002).

Bid cleavage can be induced by activation of caspase 8 (Li et al., 1998) or JNK (Yin, 2000). Alternatively, cleavage of Bid can take place downstream of the Bcl-2 action and catalyzed by caspase 3 activation (Slee et al., 2000). However, caspase 8 activation may not be absolutely required for Bid cleavage in TRO-induced apoptosis, mainly because we did not observe activation of caspase 8 despite the cleavage of Bid accompanied by cytochrome *c* release and caspase 3 activation (data not shown) after exposure of HepG2 cells to TRO. Our results show a lack of significant activation of caspase 8, which is consistent with the result of Toyoda et al. (2002), who recently reported that TRO did not activate caspase 8, whereas caspase 3 was activated in human hepatoma cells. Because we could not detect a significant activation of caspase 8 after TRO treatment, coactivation of JNK and caspase 3 seems to be responsible for Bid cleavage and the triggering of apoptosis. Our results with SP600125 (Fig. 8), in fact, are in agreement with the role of coactivation of JNK and caspase 3 in Bid cleavage. Furthermore, our results indicate that TRO-mediated response may depend on the target cell types and the agent that triggers apoptosis.

Kostrubsky et al. (2000) recently reported that TRO can be metabolized by CYP3A isozymes to its quinone metabolites, followed by sulfation and glucuronization (Ramachandran et al., 1999), and discharge into the bile duct. Another study suggested that cytochrome P450-mediated metabolism of TRO can lead to production of quinone intermediate (Yamazaki et al., 1999) or TRO ring scission pathway (Kassahun et al., 2001), before conjugation with glutathione. According to these reports, cytochrome P450 enzyme-mediated metabolism of TRO and subsequent binding of its quinone metabolites to various cellular proteins may be toxic to the cells. However, the levels of constitutively expressed CYP3A in vascular smooth muscle cells (Okura et al., 2000) and HepG2 hepatoma cells (Bai and Cederbaum, 2000) are very low compared with those in normal hepatocytes (Kostrubsky et al., 2000). Therefore, the metabolism of TRO and subsequent protein bindings by its quinone metabolites may not necessarily represent the only means of TRO-mediated cell damage. Our current results show an additional mechanism of cell death by which TRO may exert its toxicity by directly activating the JNK-related cell death pathway. In this regard, the current results are analogous to our recent report showing the critical role of the JNK-related pathway activation in the acetaminophen-induced cell death pathway (Bae et al., 2001). In this case, activation of the JNK-related cell death pathway is distinct from the previously proposed mechanism of acetaminophen-mediated cell death through the interaction of acetaminophen or its metabolites with various cellular components.

In conclusion, our data provide strong evidence that TRO causes apoptosis of human hepatoma cells by JNK activation accompanied by up-regulation of the proapoptotic proteins Bax and Bad with cleavage of Bid protein, and a reduced level of Bcl-2. In contrast, RSG neither stimulated JNK activity nor caused apoptosis of hepatoma cells. By using the

respective inhibitor of JNK or p38 kinase and DNA transfection experiments, we also demonstrated a critical role of the JNK-mediated cell death pathway in TRO-induced cell damage. The JNK-related apoptosis pathway provides a new mechanism for TRO-mediated cell damage in addition to that of the possible interaction of TRO-quinone metabolites with various cellular components.

References

Bae MA, Pie JE, and Song BJ (2001) Acetaminophen induces apoptosis of C6 glioma cells by activating the c-Jun NH$_2$-terminal protein kinase-related cell death pathway. *Mol Pharmacol* **60:**847–856.

Bai J and Cederbaum AI (2000) Overexpression of catalase in the mitochondrial or cytosolic compartment increases sensitivity of HepG2 cells to tumor necrosis factor-alpha-induced apoptosis. *J Biol Chem* **275:**19241–19249.

Beales PE, Liddi R, Giorgini AE, Signore A, Procaccini E, Batchelor K, and Pozzilli P (1998) Troglitazone prevents insulin dependent diabetes in the non-obese diabetic mouse. *Eur J Pharmacol* **357:**221–225.

Bennett BL, Sasaki DT, Murray BW, O'Leary EC, Sakata ST, Xu W, Leisten JC, Motiwala A, Pierce S, Satoh Y, et al. (2001) SP600125, an anthrapyrazolone inhibitor of Jun N-terminal kinase. *Proc Natl Acad Sci USA* **98:**13681–13686.

Chao DT and Korsmeyer SJ (1998) BCL-2 family: Regulators of cell death. *Annu Rev Immunol* **16:**395–419.

Chen Y-R, Wang X, Templeton D, Davis RJ, and Tan T-H (1996) The role of c-Jun N-terminal kinase (JNK) in apoptosis induced by ultraviolet C and gamma radiation. Duration of JNK activation may determine cell death and proliferation. *J Biol Chem* **271:**31929–31936.

Chinetti G, Griglio S, Antonucci M, Torra IP, Delerive P, Majd Z, Fruchart JC, Chapman J, Najib J, and Staels B (1998) Activation of proliferator-activated receptors α and γ induces apoptosis of human monocyte-derived macrophages. *J Biol Chem* **273:**25573–25580.

Daily D, Vlamis-Gardikas A, Offen D, Mittelman L, Melamed E, Holmgren A, and Barzilai A (2001) Glutaredoxin protects cerebellar granule neurons from dopamine-induced apoptosis by dual activation of the ras-phosphoinositide 3-kinase and Jun N-terminal kinase pathways. *J Biol Chem* **276:**21618–21626.

Day C (1999) Thiazolidinediones: a new class of antidiabetic drugs. *Diabet Med* **16:**179–192.

Engedal N and Saatcioglu F (2001) Ceramide-induced cell death in the prostate cancer cell line LNCaP has both necrotic and apoptotic features. *Prostate* **46:**289–297.

Gouni-Berthold I, Berthold HK, Weber AA, Ko Y, Seul C, Vetter H, and Sachinidis A (2001) Troglitazone and rosiglitazone induce apoptosis of vascular smooth muscle cells through an extracellular signal-regulated kinase-independent pathway. *Naunyn-Schmiedeberg's Arch Pharmacol* **363:**215–221.

Hirase N, Yanase T, Mu Y, Muta K, Umemura T, Takayanagi R, and Nawata H (1999) Thiazolidinedione induces apoptosis and monocytic differentiation in the promyelocytic leukemia cell line HL60. *Oncology* **57:**17–26.

Inanami O, Ohta T Ito S and Kuwabara M (1999) Elevation of intracellular calcium ions is essential for the H$_2$O$_2$-induced activation of SAPK/JNK but not for that of p38 and ERK in Chinese hamster V79 cells. *Antioxid Redox Signal* **1:**501–508.

Karin M (1995) The regulation of AP-1 activity by mitogen-activated protein kinases. *J Biol Chem* **270:**16483–16486.

Kassahun K, Pearson PG, Tang W, McIntosh I, Leung K, Elmore C, Dean D, Wang R, Doss G, and Bailliem TA (2001) Studies on the metabolism of troglitazone to reactive intermediates in vitro and in vivo. Evidence for novel biotransformation pathways involving quinone methide formation and thiazolidinedione ring scission. *Chem Res Toxicol* **14:**62–70.

Keelan JA, Sato TA, Marvin KW, Lander J, Gilmour RS, and Mitchell MD (1999) 15-Deoxy-Δ^{12,14}-prostaglandin J$_2$, a ligand for peroxisome proliferator-activated receptor-γ, induces apoptosis in JEG3 Choriocarcinoma cells. *Biochem Biophys Res Commun* **262:**579–585.

Kitamura S, Miyazaki Y, Shinomura Y, Kondo S, Kanayama S, and Matsuzawa Y (1999) Peroxisome proliferator-activated receptor gamma induces growth arrest and differentiation markers of human colon cancer cells. *Jpn J Cancer Res* **90:**75–80.

Kostrubsky VE, Sinclair JF, Ramachandran V, Venkataramanan R, Wen YH, Kindt E, Galchev V, Rose K, Sinz M, and Strom SC (2000) The role of conjugation in hepatotoxicity of Troglitazone in human and porcine hepatocyte cultures. *Drug Metab Dispos* **28:**1192–1197.

Lebovitz HE, Kreider M, and Freed MI (2002) Evaluation of liver function in type 2 diabetic patients during clinical trials: evidence that rosiglitazone does not cause hepatic dysfunction. *Diabetes Care* **25:**815–821.

Lee JC, Laydon JT, McDonnell PC, Gallagher TF, Kumar S, Green D, McNulty D, Blumenthal MJ, Heys JR, Landvatter SW, et al. (1994) A protein kinase involved in the regulation of inflammatory cytokine biosynthesis. *Nature (Lond)* **372:**739–746.

Lehmann JM, Moore LB, Smith-Oliver TA, Wilkison WO, Willson TM, and Kliewer SA (1995) An antidiabetic thiazolidinedione is a high affinity ligand for peroxisome proliferator-activated receptor gamma (PPARγ). *J Biol Chem* **270:**12953–12956.

Le-Niculescu H, Bonfoco E, Kasuya Y, Claret FX, Green DR, and Karin M (1999) Withdrawal of survival factors results in activation of the JNK pathway in neuronal cells leading to Fas ligand induction and cell death. *Mol Cell Biol* **19:**751–763.

Li H, Zhu H, Xu CJ, and Yuan J (1998) Cleavage of BID by caspase 8 mediates the mitochondrial damage in the Fas pathway of apoptosis. *Cell* **94:**491–501.

Mahler RJ and Adler ML (1999) Clinical review 102: type 2 diabetes mellitus: update on diagnosis, pathophysiology and treatment. *J Clin Endocrinol Metab* **84:**1165–1171.

Maroney AC, Finn JP, Bozyczko-Coyne D, O'Kane TM, Neff NT, Tolkovsky AM, Park DS, Yan CY, Troy CM, and Greene LA (1999) CEP-1347 (KT7515), an inhibitor of JNK activation, rescues sympathetic neurons and neuronally differentiated PC12 cells from death evoked by three distinct insults. *J Neurochem* **73:**1901–1912.

Ohtani KI, Shimizu H, Sato N, and Mori M (1998) Troglitazone (CS-045) inhibits β-cell proliferation rate following stimulation of insulin secretion in HIT-T 15 cells. *Endocrinology* **139:**172–178.

Okura T, Nakamura M, Takata Y, Watanabe S, Kitami Y, and Hiwada K (2000) Troglitazone induces apoptosis via the p53 and Gadd45 pathway in vascular smooth muscle cells. *Eur J Pharmacol* **407:**227–235.

Ramachandran V, Kostrubsky VE, Komoroski EJ, Zhang S, Dorko K, Esplen JE, Strom SC, and Venkataramanan R (1999) Troglitazone increases cytochrome P-450 3A protein and activity in primary cultures of human hepatocytes. *Drug Metab Dispos* **27:**1194–1199.

Slee EA, Keogh SA, and Martin SJ (2000) Cleavage of BID during cytotoxic drug and UV radiation-induced apoptosis occurs downstream of the point of Bcl-2 action and is catalysed by caspase-3: a potential feedback loop for amplification of apoptosis-associated mitochondrial cytochrome c release. *Cell Death Differ* **7:**556–565.

Soh Y, Jeong KS, Lee IJ, Bae MA, Kim YC, and Song BJ (2000) Selective activation of the c-Jun N-terminal protein kinase pathway during 4-hydroxynonenal-induced apoptosis of PC12 cells. *Mol Pharmacol* **58:**535–541.

Tafani M, Karpinich NO, Hurster KA, Pastorino JG, Schneider T, Russo MA, and Farber JL (2002) Cytochrome c release upon Fas receptor activation depends on translocation of full-length bid and the induction of the mitochondrial permeability transition. *J Biol Chem* **277:**10073–10082.

Tournier C, Hess P, Yang DD, Xu J, Turner TK, Nimnual A, Bar-Sagi D, Jones SN, Flavell RA, and Davis RJ (2000) Requirement of JNK for stress-induced activation of the cytochrome c-mediated death pathway. *Science (Wash DC)* **288:**870–874.

Toyoda M, Takagi H, Horiguchi N, Kakizaki S, Sato K, Takayama H, and Mori M (2002) A ligand for peroxisome proliferator activated inhibits cell growth and induces apoptosis in human liver cancer cells. *Gut* **50:**563–567.

Toyoda Y, Tsuchida A, Iwami E, and Miwa I (2001) Toxic effect of troglitazone on cultured rat hepatocytes. *Life Sci* **68:**1867–1876.

Watkins P and Whitcomb RW (1998) Hepatic dysfunction associated with troglitazone. *N Engl J Med* **338:**916–917.

Wilson TM, Cobb JE, Cowan DJ, Wiethe RW, Correa ID, Prakash SR, Beck KD, Moore LB, Kliewer SA, and Lehmann JM (1996) The structure-activity relationship between peroxisome proliferator-activated receptor agonism and the antihyperglycemic activity of thiazolidinediones. *J Med Chem* **39:**665–668.

Xia Z, Dickens M, Raingeaud J, Davis RJ, and Greenberg ME (1995) Opposing effects of ERK and JNK-p38 MAP kinases on apoptosis. *Science (Wash DC)* **270:**1326–1331.

Yamazaki H, Shibata A, Suzuki M, Nakajima M, Shimada N, Guengerich FP, and Yokoi T (1999) Oxidation of troglitazone to a quinone-type metabolite catalyzed by cytochrome P-450 2C8 and P-450 3A4 in human liver microsomes. *Drug Metab Dispos* **27:**1260–1266.

Yin X-M (2000) Bid, a critical mediator for apoptosis induced by the activation of Fas/TNF-R1 death receptors in hepatocytes. *J Mol Med* **78:**203–211.

Address correspondence to: Byoung J. Song, Laboratory of Membrane Biochemistry and Biophysics, National Institute on Alcohol Abuse and Alcoholism, National Institutes of Health, 12420 Parklawn Drive, Rockville, MD 20852. E-mail: bjs@mail.nih.gov